PHYSICAL REVIEW D VOLUME 19, NUMBER 9 1 MAY 1979

Solutions of simple dual bootstrap models satisfying the Lee-Veneziano relation and the smallness of cut discontinuities

Charles B. Chiu, Monowar Hossain, and Don M. Tow
Center for Particle Theory, Department of Physics, University of Texas, Austin, Texas 78712
(Received 5 July 1978)

To investigate the t-dependent solutions of simple dual bootstrap models, we discuss two general formulations, one without and one with cut cancellation for the Reggeon-particle amplitude at the planar level. We discuss the possible corresponding production mechanisms. In contrast to Bishari's formulation, both of our models recover the Lee-Veneziano relation, i.e., in the peak approximation the Pomeron intercept is unity. The solutions based on an exponential form for the reduced triple-Reggeon vertex for both models are discussed in detail. We also calculate the cut discontinuities for both of our models and for Bishari's and show that at both the planar and cylinder levels they are small compared with the corresponding pole residues. Precocious asymptotic planarity is also found in our solutions.

I. INTRODUCTION

In the past few years, the strong-interaction dynamical approach of "dual unitarization and topological expansion"[1,2] has received considerable attention. This method may be considered as the extension of the important work of Lee and Veneziano, who using certain approximations derived the interesting result that the Pomeron intercept is $\alpha_P^0 = 1$.[3-5] In the approximation of neglecting momentum-transfer, t, dependence (called peak approximation in this paper), the Lee-Veneziano formulation turns out to be the first two terms, i.e., planar plus cylinder, in the topological expansion (TE).[1] Higher-order terms are supposed to be suppressed by powers of $1/N$ [SU(N) is the internal-symmetry group], and some of these terms are further dynamically suppressed due to t-channel exoticity.

Since its introduction, much work has been done on this approach. For example, Chew and Rosenzweig[6] showed that the Pomeron-f identity is a simple realization of the TE, i.e., up to the cylinder level the Pomeron is just the f trajectory renormalized and mixed with the planar f' trajectory via the cylinder correction to the planar approximation. This Pomeron-f identity has already been shown to be a viable scheme phenomenologically.[7-9] The effects of SU(N)-symmetry breaking have been investigated.[6,7,10-12] Inclusion of baryons[13] and the next-higher-order term, the torus,[14,15] have been studied. The interesting property of asymptotic planarity was pointed out,[6,16] and elaborated on,[17-19] and its relevance to the Iizuka-Okubo-Zweig rule for decays of mesons has been investigated.[20,21]

An important ingredient in the whole approach of dual unitarization and topological expansion is the constraint of planar bootstrap, i.e., the input Regge poles should not be further renormalized by planar loop insertions, and therefore should be bootstrapped with the planar output Regge poles.[2-5,22,23] Since the input kernel is a Reggeon-Reggeon cut, a natural question that arises is does the output at the planar level contain only poles, i.e., do the Reggeon-Reggeon cuts get cancelled in the solution of the integral equation. By choosing a specific form for the inhomogeneous term, it can be shown that such cut cancellation does exist at the planar level.[24] However, the generality of such a specific choice and therefore the generality of cut cancellation has been questioned within the multi-Regge cluster framework.[25,26]

By choosing an exponential form for the reduced triple-Reggeon vertex, Bishari in an interesting paper[17] was able to investigate analytically t-dependent dual bootstrap equations up to the cylinder level. His solution gives reasonable values for the Pomeron intercept and slope, and satisfies asymptotic planarity. He also found that even if a cut-cancellation mechanism exists at the planar level, the same mechanism does not lead to cut cancellation at the cylinder level. The problem of Pomeron calculation was also recently discussed by Freeman and Zarmi.[24(b)]

However, as will be shown in the next section, Bishari's formulation does not recover in the peak approximation the nice Lee-Veneziano relation of $\alpha_P^0 = 1$. In this paper we discuss two formulations of the dual bootstrap equations, one without and one with the cut cancellation for Reggeon-particle amplitude at the planar level. We discuss the possible production mechanisms which lead to these two formulations. Both formulations, in contrast to Bishari's, recover in the peak approxi-

mation the Lee-Veneziano relation. Following Bishari's approach in solving this type of equations by choosing an exponential form for the reduced triple-Reggeon vertex, we solve these equations for the Pomeron intercept and slope. We then calculate the discontinuities of the Reggeon-Reggeon cuts at the cylinder level for both formulations and found that they are small compared with the corresponding pole residues. In the formulation where a Reggeon-Reggeon cut does exist at the planar level, this cut discontinuity also is calculated and shown to be small compared with the planar pole residue. Although planar self-consistency requires that one should also bootstrap the Reggeon-Reggeon amplitude,[24(b)] we do not pursue this investigation at this time. Also from phenomenological point of view, irrespective of whether there is cut or no cut at planar level, there will be always cut present at cylinder level, with small magnitude, as we shall see later. Finally, we provide further support for precocious asymptotic planarity,[16,17,19] i.e., the cylinder contribution is already small at $t \gtrsim 2$ GeV^2.

The theoretical formulation of the bootstrap equations, together with their solutions in integral form, is presented in Sec. II. In Sec. III, based on an exponential parametrization for the reduced triple-Reggeon vertex, we investigate the solutions, the cut discontinuities, and asymptotic planarity. Section IV ends with a short summary. Derivations of certain equations are contained in Appendix A. Modification due to the no-double-counting condition is discussed in Appendix B. In Appendix C, we compare our formulation, which incorporates the effect of finite-range interaction, with those which do not incorporate this explicitly.

II. BOOTSTRAP EQUATIONS AND THEIR SOLUTIONS IN INTEGRAL FORM

A. Bootstrap equations

The dual bootstrap equations have been discussed by many authors. However, the specific forms differ in details among authors. Here we briefly discuss our two formulations to establish our conventions, and explicitly state the assumptions involved.

First we look at the planar bootstrap equation. This is depicted in Fig. 1(a). In terms of the energy variable, it reads (we leave out writing explicitly the dependence on the overall t),

$$A_{1b}(s) = A^0_{1b}(s) + T_{1b}(s)\,, \tag{2.1}$$

with

$$T_{1b}(s) = \frac{1}{s}\int_{s_0}^{\bar{s}} ds_1 A^0_{12}(s_1) \int_{s_0}^{s} ds_2 A_{2b}(s_2) \times \int d\phi_2 \left(\frac{s}{s'_1 s_2}\right)^{\alpha_2 + \alpha_{2'}} z_2\,, \tag{2.1a}$$

where $z_2 = \cos\pi(\alpha_2 - \alpha_{2'})$ and in general $\alpha_i \equiv \alpha(t_i)$, $\alpha_{i'} \equiv \alpha(t'_i)$. In (2.1a) we choose to expand the asymptotic behavior of the Reggeon loop in powers of $(s/s'_1 s_2)$, where $s'_1 = s_1 - s_0$. This shift from the more commonly used s_1 variable to the present s'_1 variable is a simple way to get an exact factorizable kernel and at the same time satisfy the constraint of the finite-range interaction, and also (as we shall see later) to realize duality and cut cancellation associated with model II. Duality in the present context states that the appropriately weighted cluster-production contribution can be evaluated through a finite-mass sum rule (FMSR). The $A(s)$'s are the absorptive part of the various amplitudes. Subscripts i remind us that the relevant Reggeons are at α_i and $\alpha_{i'}$, and the corresponding quantities in general have t_i and t'_i dependence. The phase-space volume element, which depends on t_2 and t'_2 is denoted by $d\phi_2$. See Eq. (A1) of Appendix A for details. In Appendix C, we compare (2.1) with the case when s'_1 is replaced by s_1.

Performing the Mellin transform, we get the "effective partial-wave amplitude,"

$$A_{1b}(J) \equiv \int_{s_0}^{\infty} ds A_{1b}(s) s^{-J-1} = A^0_{1b}(J) + T_{1b}(J)\,, \tag{2.2}$$

and

$$A^0_{1b}(J) \equiv \int_{s_0}^{\infty} ds A^0_{1b}(s) s^{-J-1}\,,$$

and

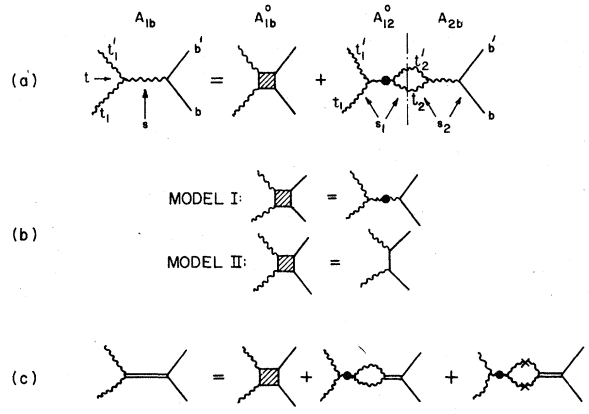

FIG. 1. Schematic illustration of the integral equations. (a) The integral equation at the planar level. (b) The inhomogeneous terms, A^0_{1b}, for models I and II. (c) The integral equation at the cylinder level.

$$T_{1b}(J) \equiv \int_{s_0}^{\infty} ds T_{1b}(s) s^{-J-1}$$
$$= \int d\phi_2 z_2 \int_{s_0}^{\bar{s}} ds_1 A_{12}^0(s_1) s_1'^{-J-1} \int_{s_0}^{\infty} ds_2 A_{2b}(s_2) s_2^{-J-1} \int_{s_2}^{\infty} \frac{ds}{s_1' s_2} \left(\frac{s}{s_1' s_2}\right)^{\alpha_2 + \alpha_{2'} - J - 2}$$
$$= \int d\phi_2 B_{12}^0 z_2 \frac{A_{2b}(J)}{J - \alpha_{c2}}, \tag{2.3}$$

where

$$\alpha_{ci} \equiv \alpha_i + \alpha_{i'} - 1, \tag{2.3a}$$

and

$$B_{12}^0 \equiv \int_{s_0}^{\bar{s}} ds_1 A_{12}^0(s_1) s_1'^{-\alpha_2 - \alpha_{2'}}. \tag{2.3b}$$

Notice B_{12}^0 is not the Mellin transform of $A_{12}^0(s_1)$ (see also Appendix B).

Up to now, the formulation is general. The different formulations mentioned at the beginning of this section correspond to different choices for the Reggeon-particle inhomogeneous term, i.e., for $A_{1b}^0(s)$ or equivalently for $A_{1b}^0(J)$. We discuss two choices. They correspond to two different production mechanisms for the end particles of the multiperipheral chain.

In model I, we assume that resonances or clusters are also produced at the two ends of the multiperipheral chain and that their average spectrum is, as that produced in the interior vertices along the multiperipheral chain, approximately given by the extrapolation of the leading Regge-pole behavior down to the low-energy region. Taking into account the most pronounced t_1 and t_1' dependence, which is due to the first nonsense-zero factor,[27] we parametrize the inhomogeneous term as

$$A_{1b}^0(s) = d_1(\alpha - \alpha_{c1})(s - s_0)^{\alpha}\, \theta(\bar{s} - s)\, \theta(s - s_0) \tag{2.4}$$

where $\alpha \equiv \alpha(t)$ and $d_1 = d(t, t_1, t_1')$, which is presumably a smooth function of t, t_1, and t_1' in the kinematic region of interest. In turn,

$$A_{1b}^0(J) \equiv f_1 g_1 \gamma_J, \tag{2.4a}$$

with

$$f_1 = 1, \quad g_1 = d_1(\alpha - \alpha_{c1}),$$

and

$$\gamma_J = \int_{s_0}^{\bar{s}} (s - s_0)^{\alpha} s^{-J-1} ds. \tag{2.4b}$$

We note that g_1 is a triple-Reggeon vertex.

Carrying out the integral explicitly, we get[28]

$$\gamma_J = \frac{s_0^{\alpha - J}}{\alpha + 1} \left(\frac{\bar{s}}{s_0} - 1\right)^{\alpha+1} \times F\left(J+1, \alpha+1; \alpha+2; -\left(\frac{\bar{s}}{s_0} - 1\right)\right). \tag{2.4c}$$

In the limit of large $\bar{s}/s_0$,[29]

$$\gamma_J \to s_0^{\alpha - J} \left(\frac{\bar{s}}{s_0} - 1\right)^{\alpha+1} \left[- \frac{1}{J - \alpha} \left(\frac{\bar{s}}{s_0}\right)^{-J-1} + \frac{\Gamma(\alpha+1)\Gamma(J-\alpha)}{\Gamma(J+1)} \left(\frac{\bar{s}}{s_0}\right)^{-\alpha-1} \right] \tag{2.4d}$$

One can explicitly check that as expected there is no pole at $J = \alpha$. For our discussion below, it suffices to know that γ_J does not contain any t_1, t_1' dependence, and it is a smooth function in t at least for $\alpha > -1$.

In model II, we assume the two end particles in the multiperipheral chain maintain the identity of the two incident particles (this we shall refer to as "the leading-particle-dominance ansatz").[30] More specifically, denoting the leading-particle mass squared by m^2, we have

$$A_{1b}^0(s) = \bar{d}_1 \delta(s - m^2), \tag{2.5}$$

and

$$A_{1b}^0(J) \equiv f_1 g_1 \gamma_J. \tag{2.5a}$$

Here as before, $g_1 = d_1(\alpha - \alpha_{c1})$, but

$$\gamma_J = \frac{\bar{d}_1}{d_1} (m^2)^{-J-1} \quad \text{and} \quad f_1 = \frac{1}{\alpha - \alpha_{c1}}. \tag{2.5b}$$

Since $\bar{d}_1$ is the direct-channel-ground-state pole residue, it is plausible that it should be a smooth function of t_1 and t_1'. Furthermore, in order for the Reggeon-Reggeon cut to cancel at the planar level, one has to assume that d_1 and $\bar{d}_1$ have the same dependences on t_1 and t_1', such that their ratio is independent of t_1 and t_1'. This will be assumed for model II for the rest of the discussion in this paper. Thus, for model II,

$$f_1 = \frac{1}{\alpha - \alpha_{c1}}, \quad g_1 = d_1(\alpha - \alpha_{c1}),$$

and

$$\gamma_J = \tilde{\gamma} (m^2)^{-J-1}, \tag{2.5c}$$

where $\tilde{\gamma}$ may depend on t. The inhomogeneous terms for models I and II are illustrated in Fig. 1(b).

If we compare the inhomogeneous terms (2.4) and (2.5) in the two models, we find that model

I has a nonsense zero in the residue function, while in model II this is absent. We recall[22] that the planar amplitude which satisfies a finite-energy sum rule (FESR) has a nonsense zero in the residue. In this sense, the inhomogeneous term of model I satisfies duality, while that of model II does not satisfy duality. This corresponds to the fact that in model I we assume cluster production, while in model II, we assume the leading-particle-dominance ansatz. We shall see in the next section that it is the very presence or absence of this nonsense zero which gives rise to cut cancellation in model II, and no cut cancellation in model I.

For both models the Reggeon-Reggeon amplitude in the kernel is assumed to take the same form. In particular, from (2.4) and (2.4b) and factorization, it is given by

$$A^0_{12}(s_1)=g_1(s_1-s_0)^{\alpha}g_2\theta(\bar{s}-s_1)\theta(s_1-s_0)\,. \tag{2.6}$$

So

$$B^0_{12}=g_1g_2\int_{s_0}^{\bar{s}}ds_1(s_1-s_0)^{\alpha-\alpha_2-\alpha_{2'}}$$

$$=g_1g_2\,\frac{(\bar{s}-s_0)^{\alpha-\alpha_{c2}}}{\alpha-\alpha_{c2}}\,, \tag{2.6a}$$

$$=g_1d_2(\bar{s}-s_0)^{\alpha-\alpha_{c2}}\equiv g_1h_2\,, \tag{2.6b}$$

where h_2 is a smooth function of t_2 and t_2'.

The result (2.6a) is just the expected FMSR result, consistent with the duality assumption stated earlier. We also mention that the $1/(\alpha-\alpha_{c2})$ factor in the same expression will be playing a crucial role in achieving the cut cancellation. This factor can be traced to be due to the coincidence of the branch point associated with the assumed Regge power behavior in $A^0_{12}(s_1)$, and the branch point of the weight factor $(s_1')^{\alpha_2+\alpha_{2'}}$. Such coincidence is expected if we associate the branch points in question with the lowest physical threshold. Within our parametrization this assumption is implicitly incorporated through the introduction of the s_1' variable in (2.1a).

To simplify the notation, we denote the partial-wave amplitude at the planar level by

$$R_i\equiv A_{ib}(J)\,.$$

Our integral equation at the planar level now takes the general form

$$R_1=f_1g_1\gamma_J+g_1\int d\phi_2\,\frac{h_2z_2R_2}{J-\alpha_{c2}}\,, \tag{2.7}$$

with $f_1=1$ for model I and $f_1=(\alpha-\alpha_{c1})^{-1}$ for model II.

For model I, since Regge behavior is assumed for both A^0_{1b} and A^0_{12}, they have common t_1 and t_1' dependences as the result of the factorization property. On the other hand, for model II, factorization is not expected in view of the leading-particle-dominance ansatz. Model II gives essentially the cut-cancellation type of models originally proposed by Bishari and Veneziano,[24] and subsequently further considered by various authors.[24-26] As these authors observed, such type of models leads to cut cancellations.

The bootstrap equation up to the cylinder level is depicted in Fig. 1(c). Denote the partial-wave amplitude for the Reggeon-particle scattering up to this level by P_1 (where the Reggeons are α_1 and $\alpha_{1'}$). Ananlogous to (2.7), for the present case,

$$P_1=f_1g_1\gamma_J+g_1\int d\phi_2\,\frac{h_2(z_2+1)P_2}{J-\alpha_{c2}}\,. \tag{2.8}$$

B. Solutions to the Bootstrap equations

Denote

$$F_J(\lambda)=\int d\phi_1\,\frac{g_1h_1z_1(\lambda)}{J-\alpha_{c1}}\,, \tag{2.9}$$

and

$$G_J(\lambda)=\int d\phi_1\,\frac{f_1g_1h_1z_1(\lambda)}{J-\alpha_{c1}}\,, \tag{2.10}$$

where $z_1(\lambda)=\cos[\lambda\pi(\alpha_1-\alpha_{1'})]$, and $\lambda=1$ and 0 corresponding to the uncrossed and crossed Reggeon loop, respectively. Note that $z_1(1)=z_1$ and $z_1(0)=1$. Also note that both $F_J(\lambda)$ and $G_J(\lambda)$ have cuts in the J plane.

From (2.7) we get

$$R_1=f_1g_1\gamma_J+\frac{g_1\gamma_JG_J(1)}{1-F_J(1)}\,. \tag{2.11}$$

The planar Regge pole occurs at $J=\alpha$, or

$$F_\alpha(1)=\int d\phi_1\,\frac{g_1h_1z_1}{\alpha-\alpha_{c1}}=1\,. \tag{2.12}$$

Equations (2.12) and (2.9) together with (2.7) give

$$R_1=f_1g_1\gamma_J+\frac{g_1\gamma_JG_J(1)}{H_J(1)(J-\alpha)}\,, \tag{2.13}$$

where

$$H_J(\lambda)=\frac{F_\alpha(\lambda)-F_J(\lambda)}{J-\alpha}$$

$$=\int d\phi_1\,\frac{g_1h_1z_1(\lambda)}{(J-\alpha_{c1})(\alpha-\alpha_{c1})}\,. \tag{2.14}$$

This is the general expression for R_1, applicable to both models I and II. In the case of model II, (2.13) simplifies. From (2.5b), $G_J(1)=H_J(1)$. In turn we get the cut-cancellation result[24,25]

$$R_1=\frac{g_1\gamma_J(J-\alpha_{c1})}{(J-\alpha)(\alpha-\alpha_{c1})}\,. \tag{2.15}$$

For the Pomeron, making use of the analogous steps leading to (2.11), we have

$$P_1 = f_1 g_1 \gamma_J + \frac{g_1 \gamma_J [G_J(1) + G_J(0)]}{1 - F_J(1) - F_J(0)} . \tag{2.16}$$

The Pomeron pole occurs at $J = \alpha_P \equiv \alpha_P(t)$, or

$$F_{\alpha_P}(1) + F_{\alpha_P}(0) = \int d\phi_1 \frac{g_1 h_1}{\alpha_P - \alpha_{c1}} (z_1 + 1) = 1 . \tag{2.17}$$

Results (2.16) and (2.17) are applicable for both models I and II, where the only difference between the two models is in the forms of G_J and γ_J.

It is instructive to recast (2.16) in a different form. We write

$$P_1 = f_1 g_1 \gamma_J + \frac{g_1 \gamma_J [G_J(1) + G_J(0)]}{(J - \alpha) H_J(1) - F_J(0)} , \tag{2.16a}$$

or

$$P_1 = f_1 g_1 \gamma_J + \frac{\gamma_J \left(1 + \frac{G_J(0)}{G_J(1)}\right) \tilde{R}_1}{1 - C_{1J} \tilde{R}_1}$$

$$= f_1 g_1 \gamma_J + \gamma_J \left(1 + \frac{G_J(0)}{G_J(1)}\right) \times (\tilde{R}_1 + \tilde{R}_1 C_{2J} \tilde{R}_2 + \tilde{R}_1 C_{2J} \tilde{R}_2 C_{3J} \tilde{R}_3 + \cdots) , \tag{2.16b}$$

where

$$\tilde{R}_1 = \frac{R_1 - f_1 g_1 \gamma_J}{\gamma_J} = \frac{g_1 G_J(1)}{(J - \alpha) H_J(1)} \tag{2.16c}$$

and

$$C_{1J} = \frac{F_J(0)}{g_1 G_J(1)} .$$

Equation (2.16b) indicates that we can also regard the Pomeron as the iteration of a suitably defined Reggeon term $\tilde{R}$, together with a suitably normalized cylinder kernel C_J.

We now verify explicitly that both models recover in the peak approximation the Lee-Veneziano relation of $\alpha_P^0 = 1$. Notice that (2.12) is applicable to both models. At $t = 0$, $t_1 = t_1'$. So $z_1(\lambda) = 1$ for both $\lambda = 1$ and $\lambda = 0$. From (2.12), in the peak approximation we have

$$\int d\phi_1 \frac{g_1 h_1}{\alpha - \alpha_{c1}} \equiv \frac{c}{\alpha_0 - \alpha_c^0} = 1 , \tag{2.18}$$

with $\alpha_0 \equiv \alpha(0)$ and $\alpha_c^0 \equiv 2\alpha_0 - 1$. So

$$c = 1 - \alpha_0 . \tag{2.19}$$

On the other hand, the Pomeron intercept is given by the zero of the denominator of the Pomeron equation (2.16a), which is again applicable for both models. It leads to

$$J - \alpha = \frac{\int d\phi_1 g_1 h_1/(J - \alpha_{c1})}{\int d\phi_1 g_1 h_1/(J - \alpha_{c1})(\alpha - \alpha_{c1})} , \tag{2.20}$$

which in the peak approximation reduces to

$$J - \alpha_0 = \frac{c/(J - \alpha_c^0)}{c/(J - \alpha_c^0)(\alpha_0 - \alpha_c^0)} = \alpha_0 - \alpha_c^0 , \tag{2.21}$$

giving the desired result

$$\alpha_P^0 = 2\alpha_0 - \alpha_c^0 = 1 . \tag{2.22}$$

We now compare our model II with that of Bishari.[17] His planar bootstrap constraint, after taking into account the relation $g_1 h_1 = g_1^2(\text{Bishari})/(\alpha - \alpha_{c1})$, is identical to our Eq. (2.12) [or (2.18) in the peak approximation]. From his Pomeron equation, his Pomeron intercept is given by

$$J - \alpha = \int d\phi_1 \frac{g_1 h_1 (\alpha - \alpha_{c1})}{J - \alpha_{c1}} , \tag{2.23}$$

which in the peak approximation becomes

$$J - \alpha_0 = \frac{c(\alpha_0 - \alpha_c^0)}{J - \alpha_c^0} \tag{2.24}$$

or

$$(J - \alpha_0)(J - \alpha_c^0) = (1 - \alpha_0) c . \tag{2.25}$$

Making use of (2.18), we find the solution to be

$$\alpha_P^0 = \frac{3\alpha_0 - 1 + \sqrt{5}(1 - \alpha_0)}{2} , \tag{2.26}$$

which gives $\alpha_P^0 \approx 0.81$, if a nominal value of $\alpha_0 = \frac{1}{2}$ is used.

For the Pomeron equation, if we compare ours, Eq. (2.21), with Bishari's Eq. (2.24), we get

$$(J - \alpha_0)_{\text{ours}} = \frac{J - \alpha_c^0}{c} \frac{c(\alpha_0 - \alpha_c^0)}{J - \alpha_c^0} = \frac{J - \alpha_c^0}{c} (J - \alpha_0)_{\text{Bishari}} . \tag{2.27}$$

We see that the difference is a factor $(J - \alpha_c^0)/c$, which from (2.18) is unity only for $J = \alpha_0$. In general, and in particular for $J = \alpha_P^0$, this factor is not unity.

III. SIMPLE SOLUTIONS, CUT DISCONTINUITIES, AND ASYMPTOTIC PLANARITY

We divide this section into three parts. In part A we discuss the Pomeron intercept and its slope, in part B we estimate the cut contribution to the amplitude at both the planar level and cylinder level, and in part C we discuss quantitatively the approach to asymptotic planarity in our models.

A. Pomeron intercept and its slope

We recall from (2.4b) and (2.6a) the quantity

$$g_1 h_1 = d_1^2 (\alpha - \alpha_{c1}) (\bar{s} - s_0)^{\alpha - \alpha_{c1}} , \tag{3.1a}$$

where as stated after (2.4) d_1 is presumably a smooth function of t, t_1, t_1'. Since $(\bar{s} - s_0)^{\alpha - \alpha_{c1}}$ is

also a smooth function of t, t_1, t_1', we parametrize the product $d_1^2(\bar{s}-s_0)^{\alpha-\alpha_{c1}}$ by an exponential and write

$$g_1 h_1 = k^2(\alpha-\alpha_{c1})e^{at+b(t_1+t_1')}\,. \tag{3.1b}$$

Here, k, a, and b are constants, and the Regge trajectory is $\alpha=\alpha_0+\alpha' t$. This form was first considered by Bishari[17] in connection with dual bootstrap equations.

For later comparison with the triple-Reggeon vertex g_{RRR} that various people have extracted from phenomenological analysis, we note that

$$g_{RRR}{}^2 \equiv g_1{}^2 = g_1 h_1(\alpha-\alpha_{c1})(\bar{s}-s_0)^{-(\alpha-\alpha_{c1})}\,. \tag{3.1c}$$

Thus

$$g_1 = k(\alpha-\alpha_{c1})(\bar{s}-s_0)^{-(\alpha-\alpha_{c1})/2} \times \exp[\tfrac{1}{2}at+\tfrac{1}{2}b(t_1+t_1')]\,. \tag{3.1d}$$

The smooth function $g_1/(\alpha-\alpha_{c1})$ is what we called the "reduced triple-Reggeon vertex."

The planar bootstrap equation (2.12) gives [see Eq. (A5) in Appendix A] Bishari's conditions,

$$\frac{Nk^2}{32\pi b}=1\,, \tag{3.2a}$$

$$a=-\tfrac{1}{2}(b+\pi^2\alpha'^2/b)\,. \tag{3.2b}$$

The conditions for output Pomeron pole, (2.17), gives [see Eq. (A10) in Appendix A]

$$1=\frac{b}{\alpha'}[\alpha_P-\alpha]\exp\left(\frac{b}{\alpha'}(\alpha_P-\alpha_c)\right)\left\{\int_1^\infty \frac{dw}{w}\exp\left[\frac{-bw}{\alpha'}(\alpha_P-\alpha_c)\right]\left[1+\exp\left(\frac{\pi^2\alpha'^2 t}{2bw}\right)\right]\right\}\,, \tag{3.3}$$

where $\alpha_c \equiv \alpha_c^0+\alpha' t/2$, with $\alpha_c^0=2\alpha_0-1$ as defined earlier.

Equation (3.3) is exact. Later in the discussion on asymptotic planarity, we will solve it by a numerical method. For now, we concentrate on the region of small t and solve the linearized version of (3.3).

For small t, (3.3) can be written as [see (A15) in Appendix A]

$$1\approx(\alpha_P-\alpha)\left\{\frac{\pi^2\alpha' t}{2}+\frac{2b}{\alpha'}\exp\left(\frac{b}{\alpha'}(\alpha_P-\alpha_c)\right)E_1\left(\frac{b}{\alpha'}(\alpha_P-\alpha_c)\right)\left[1-\frac{\pi^2\alpha' t}{4}(\alpha_P-\alpha_c)\right]\right\}\,. \tag{3.4}$$

Now assuming that in this region the Pomeron trajectory is linear in t, $\alpha_P\approx\alpha_P^0+\alpha_P' t$, we can expand the right-hand side of (3.4) in powers of t, and set the coefficient of each power to zero. This gives, up to first order in t, the following two equations (see Appendix A for details):

$$\frac{2b}{\alpha'}(\alpha_P^0-\alpha_0)\exp\left(\frac{b}{\alpha'}\tilde{p}_0\right)E_1\left(\frac{b}{\alpha'}\tilde{p}_0\right)=1 \tag{3.5a}$$

and

$$\left[\frac{\alpha_P'/\alpha'-1}{\alpha_P^0-\alpha_0}+\frac{b}{\alpha'}\left(\frac{\alpha_P'}{\alpha'}-\frac{1}{2}\right)-\frac{\tilde{p}_0\pi^2}{4}\right]E_1\left(\frac{b}{\alpha'}\tilde{p}_0\right)\exp\left(\frac{b}{\alpha'}\tilde{p}_0\right)-\frac{\alpha_P'/\alpha'-\frac{1}{2}}{\tilde{p}_0}+\frac{\pi^2}{4b/\alpha'}=0\,, \tag{3.5b}$$

where $\tilde{p}_0\equiv\alpha_P^0-\alpha_c^0$, and $E_1(x)$ is the exponential integral function.[32] This linearized approximation will later be shown to be well justified for $|t| \lesssim 0.5$ GeV^2.

For large z,[32]

$$E_1(z)\sim e^{-z}/z\,. \tag{3.6}$$

If we evaluate (3.5a) in the peak approximation, i.e., let $b\to\infty$, then (3.5a) becomes

$$2(\alpha_P^0-\alpha_0)=\tilde{p}_0=\alpha_P^0-2\alpha_0+1\,, \tag{3.7}$$

or

$$\alpha_P^0=1\,,$$

recovering the expected Lee-Veneziano relation.

We take α_0 to be its nominal value of 0.5. Then for each value of b/α', (3.5a) gives a solution for α_P^0. Then from (3.5b) one can solve for α_P'/α'. In Fig. 2(a) we plot α_P^0 and α_P'/α' versus b/α'. To make a direct comparison between α_P^0 and α_P', we plot Fig. 2(b). Some discrete values of b/α', are also shown along the curve. For example, we find that for α_P^0 increasing from 1.10 to 1.35, α_P'/α' decreases from 1.20 to 0.02.

If we choose a nominal value of 0.5 for α_P'/α' and $\alpha'=1$ GeV^{-2}, our solution gives $\alpha_P^0=1.27$ (corresponding to $b=3.2$ GeV^{-2}). In this simple model, the Pomeron intercept turns out to be a little high. However, we emphasize that our numerical result follows from the particular parametrization [see (3.1b) and (3.1c)] of g_1, the triple-Reggeon

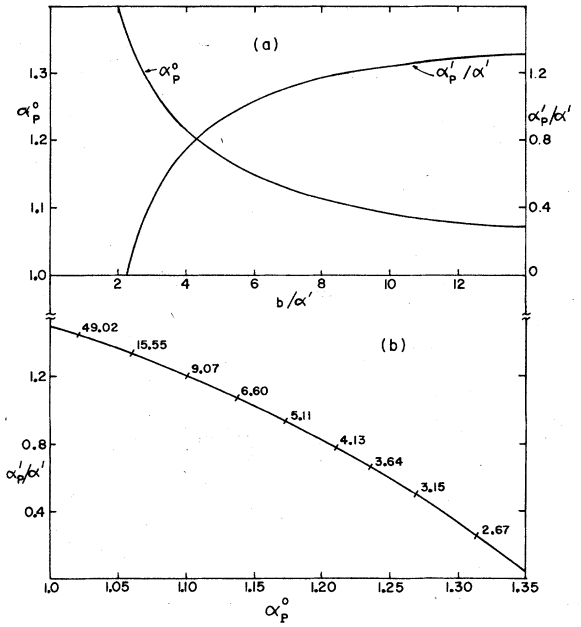

FIG. 2. (a) α_p^0 and α_p'/α' versus b/α'. (b) α_p'/α' versus α_p^0. Discrete b/α' values are labeled along the curve.

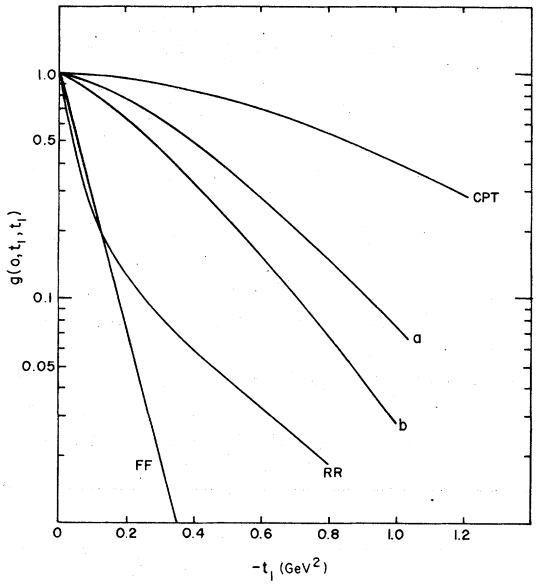

FIG. 3. Various parametrizations of the t_1 dependence of the triple-Reggeon vertex: CPT (Ref. 2), RR (Ref. 33), FF (Ref. 34), our case a and case b (see text).

vertex, which was chosen so that we can do the integrals analytically. Hopefully, with a more realistic choice for g_1, a more realistic α_P^0 emerges. The results of Ref. 19 suggest that this may indeed be the case. This problem deserves further investigation.

In Fig. 3 we plot the t_1 dependence of $g_1(0,t_1,t_1)$ at $t=0$. We choose $b=3.2$ GeV^{-2} as discussed in the previous paragraph. For $\bar{s}$, the cluster-mass cutoff, we consider two cases. Case a: $\ln(\bar{s}-s_0)\approx 1$ (or $\bar{s}\approx 3$ GeV^2); case b: $\ln(\bar{s}-s_0)\approx 2$ (or $\bar{s}\approx 6$ GeV^2). These two curves are plotted in Fig. 3 along with several other parametrizations discussed in the literature.[2,33,34] The parametrizations of Refs. 2, 33, and 34 are, respectively, $(1-1.5t_1)^{t_1}$, e^{13t_1}, and $0.8e^{18t_1}+0.2e^{3t_1}$. In these three references their parametrizations are actually for the product of g_1 and two external particle-particle-Reggeon vertices. Because of the nonleading nature of the triple-Reggeon contribution, there is large uncertainty in estimating its t_1 dependence. Notice that Ref. 2's parametrization is very much different from those of Refs. 33 and 34; this may be partly due to the differences coming from different energy ranges and different reactions considered. Our value of b/α' is well within the range of values these authors have considered.

B. Cut discontinuities

We now proceed to look at the J dependence of the amplitudes away from the pole, in particular, in the Reggeon-Reggeon-cut region. We shall calculate the discontinuities of these cuts. In this part we shall restrict ourselves to $t=0$, thus $z_1(1)=z_1(0)=1$.

We first start with model I. In this case from (2.9) and (2.10)

$$G_J^{\mathrm{I}}(\lambda)=F_J(\lambda), \tag{3.8}$$

where the superscript I denotes model I; $F_J(\lambda)$ is the same for both models and is given by (A17). Then (2.11) gives the planar partial-wave amplitude

$$R_1^{\mathrm{I}}(J)=\frac{g_1\gamma_J}{1-F_J(1)}. \tag{3.9}$$

For the partial-wave amplitude up to the cylinder level, (2.16) gives

$$P_1^{\mathrm{I}}(J)=\frac{g_1\gamma_J}{1-2F_J(1)}. \tag{3.10}$$

Next we consider model II. From (2.15) we can rewrite $R_1^{\mathrm{II}}(J)$ as

$$R_1^{\mathrm{II}}(J)=g_1\gamma_J\left(\frac{1}{\alpha_0-\alpha_{c1}}+\frac{1}{J-\alpha_0}\right). \tag{3.11}$$

Using (2.10), (2.12), and (2.14) we get

$$G_J^{\mathrm{II}}(\lambda)=H_J(\lambda)=\frac{1-F_J(\lambda)}{J-\alpha_0}. \tag{3.12}$$

From (2.16) and (3.12), the corresponding partial-wave amplitude up to the cylinder level is given by

$$P_1^{II}(J) = g_1\gamma_J\left[\frac{1}{\alpha_0-\alpha_{c1}} + \frac{2[1-F_J(1)]}{(J-\alpha_0)[1-2F_J(1)]}\right]$$
$$= g_1\gamma_J\left[\frac{1}{\alpha_0-\alpha_{c1}} + \frac{1}{J-\alpha_0} + \frac{1}{(J-\alpha_0)[1-2F_J(1)]}\right]. \quad (3.13)$$

As discussed in Appendix A, the function $F_J(1)$ has a cut in the J plane along the real axis for $-\infty < J \leq \alpha_c$. Therefore, the amplitudes $R_1^I(J)$, $P_1^I(J)$, and $P_1^{II}(J)$ also have these cuts, and we want to calculate the discontinuities across these cuts. In view of (3.11), $R_1^{II}(J)$ has no cut.

Since we will compare the cut discontinuity with the pole residue, we work with a normalized partial-wave amplitude $\tilde{A}(J)$, where $\tilde{A}(J)$ is normalized such that the Pomeron residue is unity. The discontinuity of $\tilde{A}(J)$ is defined as

$$\Delta(J) = (1/2i)[\tilde{A}(J+i\epsilon) - \tilde{A}(J-i\epsilon)]. \quad (3.14)$$

In all cases considered $\tilde{A}$ has the general form

$$\tilde{A}(J) = \frac{B}{D_R + iD_I} + C,$$

where B and C are regular in J, and D_R and D_I are real quantities. Therefore,

$$\Delta(J) = \frac{-BD_I}{D_R^2 + D_I^2}. \quad (3.15)$$

To compare with Bishari's work,[17] we note that his Pomeron amplitude P^B is given by

$$P^B(J) = \frac{\text{constant}}{J-\alpha_0-(1+\alpha'/b-J)-(b/\alpha')(J-\alpha_0)^2\exp[(b/\alpha')(J-\alpha_c)]E_1((b/\alpha')(J-\alpha_c))}. \quad (3.16)$$

From the discontinuity of the $E_1(z)$ function [Eq. (A18)], the discontinuities in our models as well as in Bishari's model can then be easily calculated.

We plot in Fig. 4 the discontinuities for R_1^I, P_1^I, P_1^{II}, and P^B as a function of J from the branch point $J = 0$ down to -1.

Near the branch point $J = \alpha_c^0 = 0$, Δ_P^B is the largest, and Δ_P^I and Δ_P^{II} are comparable. For the latter two, from (3.10) and (3.13) and the normalization convention for Δ, there is the relation

$$\Delta_P^{II} = \frac{\alpha_P^0 - \alpha_0}{J-\alpha_0}\Delta_P^I.$$

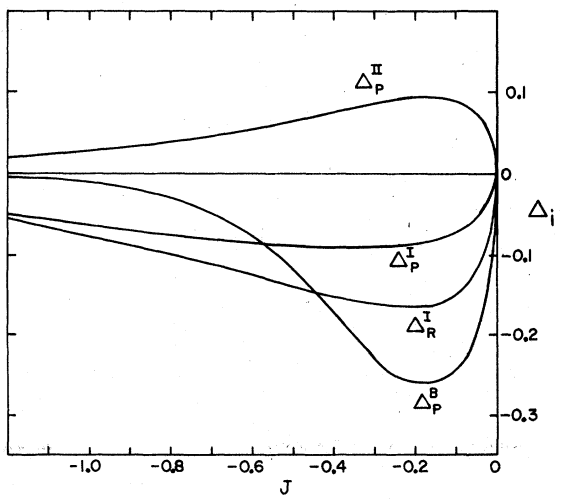

FIG. 4. The normalized discontinuity functions versus J. See text for the definitions of the various Δ's.

The corresponding power behavior in the full amplitude associated with the discontinuity in the partial-wave amplitude at J is s^J (when applied to an internal link in a multiperipheral chain, s should be replaced by the subenergy $s_{i,i+1}$). Because the tip of the cut lies approximately $\frac{1}{2}$ and 1 unit below the Reggeon and Pomeron poles, respectively, the cut contribution is already much suppressed by this energy factor.

Now we want to show that even without taking into account this energy factor, the area under the cut discontinuity function shown is already significantly less than the pole contribution in the same partial-wave amplitude. More precisely, we consider the ratio

$$\eta = I_c/\pi r,$$

where for definiteness we take

$$I_c = \int_{\alpha_c^0-1}^{\alpha_c^0} dJ\Delta(J),$$

and it is to be compared with the pole contribution in the same amplitude given by πr, with r being the pole residue. For the Pomeron amplitude, by construction the residue of the pole is $r = 1$. For the Reggeon in R^I, its pole residue is $r = 0.48$. We then find $\eta = 0.08$, 0.03, 0.02, and 0.04 for R^I, P^I, P^{II}, and P^B, respectively. Thus, the contribution of the cut is indeed very negligible both at the planar and at the cylinder levels.

C. Asymptotic planarity

Here we investigate the asymptotic planarity in our model. Equation (3.3) can be rewritten as

$$1=\frac{b}{\alpha'}X\exp\left(\frac{b}{\alpha'}(X+1-\alpha_0+\tfrac{1}{2}\alpha' t)\right)\int_1^\infty\frac{dw}{w}\exp\left(-\frac{bw}{\alpha'}(X+1-\alpha_0+\tfrac{1}{2}\alpha' t)\right)\left[1+\exp\left(\frac{\pi^2\alpha'^2 t}{2bw}\right)\right]. \tag{3.17}$$

where $X\equiv\alpha_P-\alpha$.

It is instructive to compare the planar and the cylinder contributions in the integrand. Note that the planar contribution has an extra factor of $\exp(\pi^2\alpha'^2 t/2bw)$, which stems from the planar Reggeon phase factors. This extra factor grows exponentially with t, in the positive-t region, resulting in the dominance of the planar term, or asymptotic planarity. On the other hand, in the negative-t region, the same factor gives a relative suppression for the planar contribution.

Using (3.6) and (A13), after some algebra (3.17) gives

$$X=\alpha_P-\alpha<\text{const}\times(1-\alpha_0+\tfrac{1}{2}\alpha' t)\exp\left(\frac{-\pi^2\alpha'^2 t}{2b}\right), \tag{3.18}$$

which gives the rate of the approach to asymptotic planarity. A behavior similar to (3.18) was already given in Ref. 17.

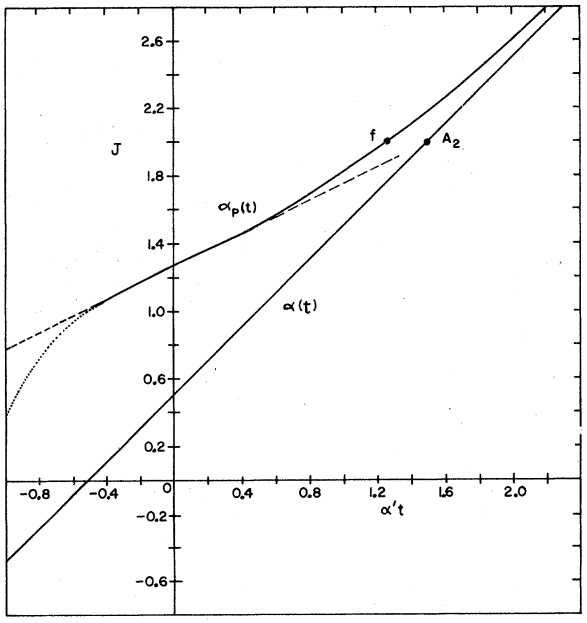

FIG. 5. The calculated Pomeron trajectory function in a Chew-Frautschi plot. The dashed curve is obtained based on the linear approximation discussed in Sec. III A. The solid curve is obtained by the numerical calculation of Sec. III C. The planar Reggeon trajectory is given by $\alpha=0.5+\alpha' t$. The f and A_2 are the spin-2 particles. The form of α_P for $t<-0.5$ GeV^2 depends more sensitively on the parametrization used for the triple-Reggeon vertex (see text).

To get a detailed picture of the t dependence of the trajectory α_P, we solve X numerically from (3.17). The resultant α_P, together with the input Reggeon trajectory $\alpha=\frac{1}{2}+\alpha' t$, is plotted in Fig. 5.

We see that for $|t|\lesssim 0.5$ GeV^2, the Pomeron trajectory is approximately linear and thus justifies the linear approximation used previously [see (3.5a) and (3.5b)] to solve for α_P^0 and α_P' at $t=0$. We find that the error in $(\alpha_P-\alpha)$ is $\lesssim 4\%$ in this range of t.

As usual if we identify the A_2 and f mesons to be the spin-2 particles on the α and α_P trajectories, respectively, our curves give

$$M_{A_2}{}^2-M_f{}^2\approx 0.2\ \text{GeV}^2,$$

(where we set $\alpha'=1$ GeV^{-2}), while the experimental value is 0.1 GeV^2.

It is remarkable that the predicted value is of the right sign and within a factor of 2 of the experimental value. Note that a lower α_P^0 may make the agreement even better.

The positive-t behavior of α_P shown here is very similar to the result of Tsou,[19] who instead of solving the integral equations, iterated up to eleven loops and also used a different parametrization for the triple-Reggeon vertex. This indicates that this positive-t behavior is relatively insensitive to different parametrizations for $g_1(t,t_1,t_1')$. On the other hand, for $t\lesssim -0.5$ GeV^2 our α_P bends downward, whereas hers stays up. We attribute this difference to be due to the different parametrizations used for g_1. For this reason, in this region α_P is indicated by a dotted line in Fig. 5.

IV. SUMMARY

We have presented two formulations of the dual bootstrap equations for the Reggeon-particle amplitude: one without and one with cut cancellation at the planar level. Both formulations in the peak approximation recover the Lee-Veneziano relation of $\alpha_P^0=1$. Choosing an exponential form for the reduced triple-Reggeon vertex, we solved these equations. We showed how the discontinuities of the Reggeon-Reggeon cuts can be calculated. We found that at the cylinder level, the cut discontinuity in both models (and also in Bishari's) is small compared with the Pomeron-pole residue. Even though in model I the Reggeon-Reggeon cut is not cancelled at the planar level, we found that

its discontinuity is small compared with the planar-pole residue. This important result indicates that the planar-pole bootstrap constraint can be satisfied to a good approximation even if there is no cut-cancellation mechanism. We provided further quantitative support for precocious asymptotic planarity in the positive-t region; we also found that in the large negative-t region, α_P depends more sensitively on the parametrization of the triple-Reggeon vertex.

Note added. For completeness, we include here a brief discussion for the Reggeon-Reggeon case. We recall that the distinction between models I and II lies in the choice of the production mechanism of the leading particle (i.e., the end particle along the multiperipheral chain). Since the Reggeon-Reggeon amplitude never involves the leading particle (which by definition is joined on to the external particles), the bootstrap equations for the Reggeon-Reggeon amplitude are identical in both cases. From the definition of the kernel given in (2.6), the Reggeon-Reggeon integral equation analogous to (2.7) is given by

$$R_{13}=g_1g_3\gamma_J+g_1\int d\phi_2\frac{g_2h_2z_2R_{23}}{J-\alpha_{c2}},$$

with γ_J defined in (2.4b). Analogous to (2.13), the solution is given by

$$R_{13}=g_1g_3\gamma_J+\frac{g_1g_3\gamma_J}{J-\alpha}\times\frac{\int d\phi_2 g_2h_2z_2/(J-\alpha_{c2})}{\int d\phi_2 g_2h_2z_2/(J-\alpha_{c2})(\alpha-\alpha_{c2})}.$$

R_{13} is symmetric with respect to the indices 1 and 3, as expected. Notice that the Reggeon-loop integrations in both numerator and denominator correspond to cuts in J plane. There is no cut cancellation here.

Since the completion of this work, the results of including the $t_{\min}$ effects and of avoiding the double counting have been calculated[35] and found to give a lower value of the Pomeron intercept (closer to one) and also a reasonable value for the slope.

ACKNOWLEDGMENT

This work was supported in part by the U. S. Energy Research Development Administration under Contract No. E(40-1)3992.

APPENDIX A: THE $F_J(\lambda)$ FUNCTIONS, REGGEON, AND POMERON CONSTRAINT CONDITIONS

We recall that the $F_J(\lambda)$ functions are defined as

$$F_J(\lambda)=\int d\phi_1\frac{g_1h_1z_1(\lambda)}{J-\alpha_{c1}}, \tag{2.9}$$

where $\lambda=1$ or 0, $z_1(1)\equiv\cos\pi(\alpha-\alpha_1')$, and $z_1(0)=1$. In this Appendix we give the derivations of $F_J(1)$ and $F_J(0)$ for the parametrization considered in Sec. III,

$$g_1h_1=k^2(\alpha-\alpha_{c1})\exp[at+b(t_1+t_1')]. \tag{3.1b}$$

For completeness, we will also include the details leading to the Reggeon condition (3.2) and the Pomeron equations (3.3) and (3.5).

The two-body phase-space volume element is given by

$$d\phi_1\equiv\frac{N}{16\pi^2}dt_1dt_1'\frac{\theta(K)}{\sqrt{K}}. \tag{A1}$$

In high-energy small-angle approximation,[36]

$$\frac{\theta(K)}{\sqrt{K}}\approx\frac{\pi}{s}\sum_l(2l+1)P_l(\cos\theta)P_l(\cos\theta_1)P_l(\cos\theta_1')\approx\frac{\pi}{2}\int_0^\infty db\,bJ_0(bw)J_0(bu)J_0(bv), \tag{A2}$$

where $u^2=-t_1$, $v^2=-t_1'$, and $w^2=-t$. The factor N is associated with the SU(N) symmetry assumed. For a planar loop, N is the number of windows. On the other hand, for the cylinder loops, N is present only when the crossed channel is an SU(N) singlet. This is the case in the present work.

We start with the following two triple-Fourier-Bessel-transform identities. Let $z=x+iy$.

$$I(x,y)\equiv\langle e^{-zu^2}e^{-z^*v^2}\rangle\equiv\int_0^\infty db\,bJ_0(bw)\int_0^\infty du\,ue^{-zu^2}J_0(bu)\int_0^\infty dv\,ve^{-z^*v^2}J_0(bv)$$
$$=\int_0^\infty db\,bJ_0(bw)\frac{1}{4zz^*}\exp\left(-\frac{x}{2zz^*}b^2\right)$$
$$=\frac{1}{4x}\exp\left[\frac{1}{2}\left(x+\frac{y^2}{x}\right)t\right]. \tag{A3}$$

Notice that $I(x,y)$ is real and it is an even function of y. Also,

$$I(x,y;p)\equiv\left\langle\ \frac{e^{-zu^2-z^*v^2}}{p+u^2+v^2}\ \right\rangle = e^{px}\int_x^\infty dx'\langle\exp[-(p+u^2+v^2)x']\exp[-iy(u^2-v^2)]\rangle$$

$$= e^{px}\int_x^\infty \frac{dx'}{4x'}\exp[-(p-\tfrac{1}{2}t)x']\exp\left(\frac{y^2}{2x'}t\right), \tag{A4}$$

where $p-t/2>0$. Again $I(x,y;p)$ is real and it is an even function of y. Both identities are obtained through integrations over negative t_1 and t_1' regions. Thus, t is confined to the region $t\leq 0$. The I's will be analytically continued to the positive-t region.

Now we evaluate $F_\alpha(1)$. From (2.9), (3.1b), and (A3) we get

$$F_\alpha(1)=\frac{Nk^2}{8\pi}e^{at}\langle\exp[-b(u^2+v^2)]\cos\pi\alpha'(u^2-v^2)\rangle$$

$$=\frac{Nk^2}{8\pi}e^{at}I(b,\pi\alpha')=\frac{Nk^2}{32\pi b}\exp\left[\left(a+\frac{b}{2}+\frac{(\pi\alpha')^2}{2b}\right)t\right]. \tag{A5}$$

This leads to (3.2).

For general J, from (2.9) and (3.1b),

$$F_J(1)=\frac{Nk^2}{8\pi}e^{at}\,\mathrm{Re}\left\langle\left(1-\frac{J-\alpha}{J-\alpha_{c1}}\right)\exp[-(b+i\pi\alpha')u^2]\exp[-(b-i\pi\alpha')v^2]\right\rangle$$

$$=1-\frac{Nk^2}{8\pi\alpha'}e^{at}(J-\alpha)\left\langle\frac{e^{-zu^2}e^{-z^*v^2}}{p+u^2+v^2}\right\rangle, \tag{A6}$$

with

$$p=(1/\alpha')(J-2\alpha_0+1),\quad x=b,\quad \text{and } y=\pi\alpha',\quad z=x+iy. \tag{A6a}$$

And

$$F_J(0)=\frac{Nk^2}{8\pi}e^{at}\langle\exp[-b(u^2+v^2)]\rangle-\frac{Nk^2}{8\pi\alpha'}e^{at}(J-\alpha)\left\langle\frac{\exp[-b(u^2+v^2)]}{p+u^2+v^2}\right\rangle. \tag{A7}$$

Making use of (A3) to (A5) we can rewrite (A6) and (A7) as

$$F_J(1)=1-\frac{b}{\alpha'}\exp\left(\frac{-\pi^2\alpha'^2t}{2b}\right)(J-\alpha)\exp\left(\frac{b}{\alpha'}(J-\alpha_c)\right)\int_1^\infty\frac{dw}{w}\exp\left(\frac{-b}{\alpha'}(J-\alpha_c)w\right)\exp\left(\frac{\pi^2\alpha'^2t}{2bw}\right) \tag{A8}$$

and

$$F_J(0)=\exp\left(\frac{-\pi^2\alpha'^2t}{2b}\right)\left[1-\frac{b}{\alpha'}(J-\alpha)\exp\left(\frac{b}{\alpha'}(J-\alpha_c)\right)\int_1^\infty\frac{dw}{w}\exp\left(\frac{-b}{\alpha'}(J-\alpha_c)w\right)\right]. \tag{A9}$$

From (A8), (A9), and (2.17), the Pomeron condition gives

$$1=\frac{b}{\alpha'}(\alpha_P-\alpha)\exp\left(\frac{b}{\alpha'}(\alpha_P-\alpha_c)\right)\int_1^\infty\frac{dw}{w}\exp\left(\frac{-b}{\alpha'}(\alpha_P-\alpha_c)w\right)\left[1+\exp\left(\frac{\pi^2\alpha'^2t}{2bw}\right)\right], \tag{A10}$$

which is Eq. (3.3).

To proceed further, we make use of the exponential integral function defined by[32]

$$E_n(z)=\int_1^\infty dt e^{-zt}/t^n,\quad n=0,1,2,\ldots, \tag{A11}$$

which satisfy the recursion relation

$$E_{n+1}(z)=(1/n)[e^{-z}-zE_n(z)]. \tag{A12}$$

We can now rewrite (A9) as

$$F_J(0)=\exp\left(\frac{-\pi^2\alpha'^2t}{2b}\right)\left[1-\frac{b}{\alpha'}(J-\alpha)\exp\left(\frac{b}{\alpha'}(J-\alpha_c)\right)E_1\left(\frac{b}{\alpha'}(J-\alpha_c)\right)\right]. \tag{A13}$$

For small t, the last factor $\exp(\pi^2\alpha'^2t)/2bw)$ in (A8) can be expanded, and (A8) becomes

$$F_J(1)\approx 1-\exp\left(\frac{-\pi^2\alpha'^2t}{2b}\right)(J-\alpha)\left[\frac{\pi^2\alpha't}{2}+\frac{b}{\alpha'}\exp\left(\frac{b}{\alpha'}(J-\alpha_c)\right)\left(1-\frac{\pi^2\alpha't}{2}(J-\alpha_c)\right)E_1\left(\frac{b}{\alpha'}(J-\alpha_c)\right)\right]. \tag{A14}$$

In this small-t approximation, the Pomeron condition $1 = F_{\alpha P}(1) + F_{\alpha P}(0)$ becomes

$$1 = (\alpha_P - \alpha)\left[\frac{\pi^2\alpha' t}{2} + \frac{2b}{\alpha'}\exp\left(\frac{b}{\alpha'}(\alpha_P - \alpha_c)\right) E_1\left(\frac{b}{\alpha'}(\alpha_P - \alpha_c)\right)\left(1 - \frac{\pi^2\alpha' t}{4}(\alpha_P - \alpha_c)\right)\right] + O(t^2), \tag{A15}$$

which is Eq. (3.4). Setting $\alpha_P \approx \alpha_P^0 + \alpha_P' t$ and expanding the right-hand side of (A15) in powers of t, and using $E_1(z + \Delta z) \approx E_1(z) - (e^{-z}/z)\Delta z$, we get

$$1 = (\alpha_P^0 - \alpha_0)\left(1 + \frac{\alpha_P' - \alpha'}{\alpha_P^0 - \alpha_0} t\right)\left\{\frac{\pi^2\alpha' t}{2} + \frac{2b}{\alpha'}\left[1 + bt\left(\frac{\alpha_P'}{\alpha'} - \frac{1}{2}\right) - \frac{\pi^2\alpha' t}{4}\tilde{p}_0\right]\right.$$
$$\left. \times \left[\exp\left(\frac{b}{\alpha'}\tilde{p}_0\right) E_1\left(\frac{b}{\alpha'}\tilde{p}_0\right) + \frac{t(\alpha'/2 - \alpha_P')}{\tilde{p}_0}\right]\right\} + O(t^2), \tag{A16}$$

where $\tilde{p}_0 \equiv \alpha_P^0 - \alpha_c^0$. This gives the Pomeron conditions (3.5a) and (3.5b) of text.

From (A13) and (A14) note that at $t = 0$, we get

$$F_J(1) = F_J(0) = 1 - \frac{b}{\alpha'}(J - \alpha_0)\exp\left(\frac{b}{\alpha'}(J - \alpha_c^0)\right) E_1\left(\frac{b}{\alpha'}(J - \alpha_c^0)\right). \tag{A17}$$

The function $E_1(z)$ has a cut in the z plane along the negative real axis. Setting $z = u + iv$, the cut is from $u = -\infty$ to 0. The complex value of $E_1(z)$ just above and below the cut is given by

$$E_1(-u \pm i\epsilon) = -\mathrm{Ei}(u) \mp i\pi, \quad u > 0 \tag{A18}$$

where

$$\mathrm{Ei}(u) = -\mathrm{p}\int_{-u}^{\infty} \frac{e^{-t}}{t} dt, \quad u > 0$$
$$= \gamma_0 + \ln u + \sum_{n=1}^{\infty} \frac{u^n}{n!n}, \tag{A19}$$

with the Euler constant $\gamma_0 = 0.577\ldots$. From (A13) and (A14) we see that $F_J(0)$ and $F_J(1)$ have a cut in J for $-\infty < J \leq \alpha_c$. In calculating $E_1(u)$ for positive argument, we have used the approximate formula (5.1.54) of Ref. 32. For the negative argument, the above series expansion is used.

APPENDIX B: MODIFICATIONS DUE TO THE NO-DOUBLE-COUNTING CONDITION

For completeness we mention that it is straightforward to incorporate the no-double-counting condition for the planar integral equation formulated in the energy plane (see, e.g., the particular version discussed recently by Freeman, Zarmi, and Veneziano[24(c)]). In terms of our notations, this condition states that

$$s_0 < s_1 < \bar{s} \quad \text{and} \quad s_0 < s_2 < s s_0/\bar{s}. \tag{B1}$$

Thus, analogous to (2.1a), we now have

$$T_{1b}(s) = \frac{1}{s}\int_{s_0}^{\bar{s}} ds_1 A_{12}^0(s_1) \int_{s_0}^{s s_0/\bar{s}} ds_2 A_{2b}(s_2) \times \int d\phi_2 \left(\frac{s}{s_1' s_2}\right)^{\alpha_2 + \alpha_2'} z_2. \tag{B2}$$

The corresponding partial-wave amplitude is given by

$$T_{1b}(J) = \int d\phi_2 z_2 \int_{s_0}^{\bar{s}} ds_1 A_{12}^0(s_1) s_1'^{-\alpha_2 - \alpha_2'} \times \left(\frac{\bar{s}}{s_0}\right)^{\alpha_2 + \alpha_2' - J - 1} \frac{A_{2b}(J)}{J - \alpha_{c2}}$$
$$= \int d\phi_2 \frac{B_{12}^0 z_2 A_{2b}(J)}{J - \alpha_{c2}}. \tag{B3}$$

Thus, instead of (2.6a), we have

$$B_{12}^0 = \int_{s_0}^{\bar{s}} ds_1 A_{12}^0(s_1) s_1'^{-\alpha_2 - \alpha_2'} \left(\frac{\bar{s}}{s_0}\right)^{\alpha_{c2} - J} \equiv g_1 h_2, \tag{B4}$$

with

$$h_2 = g_2 \frac{(\bar{s} - s_0)^{\alpha - \alpha_{c2}}}{\alpha - \alpha_{c2}} \left(\frac{\bar{s}}{s_0}\right)^{\alpha_{c2} - J}$$
$$\equiv d_2 (\bar{s} - s_0)^{\alpha - \alpha_{c2}} \left(\frac{\bar{s}}{s_0}\right)^{\alpha_{c2} - J}. \tag{B5}$$

We see that imposing this no-double-counting condition amounts to redefining h_2, which now contains an extra slowly varying multiplicative factor $(\bar{s}/s_0)^{\alpha_{c2} - J}$. It is interesting to note that in the leading order of $s_0/\bar{s}$, h_2 reduces to

$$h_2 = d_2 s_0^{J - \alpha_{c2}} \bar{s}^{J - \alpha}. \tag{B6}$$

Hence, h_2 is independent of $\bar{s}$ at $J = \alpha$, and the planar bootstrap condition (2.12) is independent of cluster size $\bar{s}$, as it is expected[24(c)] from no-double-counting condition (B1).

In the case of Pomeron, there is no restriction due to double counting, and our derivation in the text remains unaltered.

APPENDIX C: FINITE-RANGE ANALYTICITY AND S_1-S_2 SYMMETRIC FORMULATION

Our integral equation (2.1) [or (B2)] is formulated with the explicit inclusion of finite threshold energy $\sqrt{s_0}$. This is motivated by the fact that, in the Froissart-Gribov projection of the t-channel partial-wave amplitude, there is a gap between the branch point of the weight function, the second-kind Legendre function, and the lowest s-channel singularity. This gap reflects the finite-range nature of strong interaction. We shall refer to the incorporation of this finite gap as the "finite-range analyticity" requirement. To impose this requirement and obtain desired kernels, our integral equations involve the s_1' variable, so variables s_1 and s_2 are not treated on a symmetric footing.

What is the effect of this asymmetric formulation? One can easily check that our kernel B_{12}^0 given in Eq. (2.3b) and the corresponding expression obtained when replacing s_1' by s_1 are the same to leading power in $(\bar{s}/s_0)$. So this asymmetry only induces corrections in lower order of $(\bar{s}/s_0)$. This is acceptable, since correction of the same order is also expected from the very asymptotic expansion used in deriving the integral equation.

Nevertheless, one might still want to ask whether it is possible to write down the integral equation and to arrive at the desired kernel starting from a manifestly s_1-s_2 symmetric framework. This possibility has been investigated previously (see, for example, Ref. 22). However, to our knowledge one has achieved this only at the expense of neglecting the finite-range analyticity requirement. For completeness, we include below a brief discussion for this s_1-s_2 symmetric formulation. The purpose of our discussion here is merely to illustrate those essential approximations involved in arriving at the desired kernel. Most approximations enumerated have also been implicitly assumed for the derivation of the kernel used in the text.

We begin with the expression similar to the one given in Ref. 24(c),

$$T_{1b}(s)=\frac{1}{s}\int d\phi_2 z_2 \int_0^{\bar{s}} ds_1 A_{12}^0(s_1) \times \int_0^{as/\bar{s}} ds_2 A_{2b}\left(\frac{s}{s_1 s_2}\right)^{\alpha_2+\alpha_2'}, \tag{C1}$$

where "a" is a scale factor. Here the approximation of replacing the transverse mass-squared $s_{iT}=s_i+p_{Ti}^2$ by s_i has already been made. Notice the right-hand side would be completely symmetric with respect to s_1 and s_2, if one were to set $\bar{s}=\sqrt{as}$. For present consideration, $\bar{s}$ is large, but it is independent of s. Since the lower limits start from zero, the finite-range analyticity requirement is ignored here. A careful application of the Steinmann relation[37] reveals that one should write A_{12}^0 in the following form:

$$A_{12}^0(s_1)=s_1^{\alpha_1+\alpha_1'+\alpha_2+\alpha_2'}\frac{1}{2i}\Delta_{s_1}U_{12}. \tag{C2}$$

For our present discussion, it suffices to specify that the function U_{12} has only right-hand discontinuity in s_1. And again setting $p_{iT}=0$, the Regge asymptotic behavior of U_{12} is given by

$$U_{12}\sim g_1 g_2 (e^{-i\pi}s_1)^{\alpha-\alpha_1-\alpha_1'-\alpha_2-\alpha_2'}, \tag{C3}$$

where g_1 and g_2 are triple-Regge-vertex functions. Making use of the above expressions, one finds the corresponding kernel is given by

$$\begin{aligned} B_{12}^0 &= \int_0^{\bar{s}} ds_1 A_{12}^0(s_1) s_1^{-\alpha_2-\alpha_2'} \\ &\approx -g_1 g_2 \sin\pi(\alpha-\alpha_1-\alpha_1'-\alpha_2-\alpha_2')\frac{\bar{s}^{\alpha-\alpha_{c2}}}{\alpha-\alpha_{c2}} \\ &\approx [-g_1\sin\pi(\alpha_1+\alpha_1')]g_2\frac{\bar{s}^{\alpha-\alpha_{c2}}}{\alpha-\alpha_{c2}}. \end{aligned} \tag{C4}$$

In the last step the pole-dominance approximation is made, which amounts to evaluating the numerator at $\alpha=\alpha_{c2}$. Thus, we arrive at the desired kernel (2.3b) with the appropriate pole denominator and factorizable residue as that used in the text.

[1] G. Veneziano, Phys. Lett. 52B, 220 (1974); Nucl. Phys. B74, 365 (1974).

[2] H.-M. Chan, J. E. Paton, and S. T. Tsou, Nucl. Phys. B86, 479 (1975); H.-M. Chan, J. E. Paton, S. T. Tsou, and S. W. Ng, *ibid.* B92, 13 (1975).

[3] H. Lee, Phys. Rev. Lett. 30, 719 (1973).

[4] G. Veneziano, Phys. Lett. 43B, 413 (1973).

[5] See also, H.-M. Chan and J. E. Paton, Phys. Lett. 46B 228 (1973).

[6] G. F. Chew and C. Rosenzweig, Phys. Lett. 58B, 93 (1975); Phys. Rev. D 12, 3907 (1975).

[7] C. B. Chiu, M. Hossain, and D. M. Tow, Phys. Rev. D 14, 3141 (1976).

[8] P. R. Stevens, G. F. Chew, and C. Rosenzweig, Nucl. Phys. B110, 355 (1976).

[9] C. B. Chiu and D. M. Tow, Nucl. Phys. B137, 137 (1978).

[10] N. Papadopoulos, C. Schmid, C. Sorensen, and D. M. Webber, Nucl. Phys. B101, 189 (1975).

[11]K. Knoishi, Nucl. Phys. B116 356 (1976).
[12]R. Anderson and G. C. Joshi, Phys. Rev. D 15, 1387 (1977).
[13]H.-M. Chan and S. T. Tsou, Nucl. Phys. B118, 413 (1977).
[14]H.-M Chan, K. Konishi, J. Kwiecinski, and R. G. Roberts, Phys. Lett. 63B, 441 (1976).
[15]M. Bishari, Phys. Lett. 64B, 203 (1976).
[16]G. F. Chew and C. Rosenzweig, Nucl. Phys. B104, 290 (1976).
[17]M. Bishari, Phys. Lett. 59B, 461 (1975).
[18]H.-M. Chan *et al.*, Phys. Lett. 64B, 301 (1976).
[19]S. T. Tsou, Phys. Lett. 65B, 81 (1976).
[20]H.-M. Chan, J. Kwiecinski, and R. G. Roberts, Phys. Lett. 60B, 367 (1976); H.-M. Chan *et al.*, *ibid.* 60B, 469 (1976).
[21]C. Rosenzweig, Phys. Rev. D 13, 3080 (1976).
[22]C. Rosenzweig and G. Veneziano, Phys. Lett. 52B, 335 (1974).
[23]M. M. Schaap and G. Veneziano, Lett. Nuovo Cimento 12, 204 (1975).
[24](a) M. Bishari and G. Veneziano, Phys. Lett. 58B, 445 (1975).
(b) J. R. Freeman and Y. Zarmi, Nucl. Phys. B112, 303 (1976).
(c) J. R. Freeman, Y. Zarmi, and G. Veneziano, Nucl. Phys. B120, 477 (1977).
[25]S. Feinberg and D. Horn, Tel-Aviv Report No. TAUP-511-76, 1976 (unpublished).
[26]J. Kwiecinski and N. Sakai, Nucl. Phys. B127, 87 (1977).
[27]Take, for example, the dual resonance model. The absorptive part A_{1b} of the Reggeon-particle amplitude is proportional to

$$\mathrm{Im}V(\alpha_s,\bar{\alpha}_1)=\mathrm{Im}\left[\frac{\Gamma(-\alpha_s)(\Gamma(-\bar{\alpha}_1)}{\Gamma(-\alpha_s-\bar{\alpha}_1)}\right],$$

with $\bar{\alpha}_1=\alpha-\alpha_1-\alpha_1'$. For large α_s,

$$A_{1b}\propto\mathrm{Im}V\to\frac{\alpha_s^{\bar{\alpha}_1}}{\Gamma(\bar{\alpha}_1+1)}.$$

So the first nonsense zero is at $\bar{\alpha}_1=-1$, or $\alpha=\alpha_1+\alpha_1,-1=\alpha_{c1}$.

[28]We have used the identity (see p. 284 of Ref. 31)

$$\int_0^u\frac{x^{p-1}}{(1+qx)^a}=\frac{u^p}{p}F(a,p;p+1;-qu),$$

where F is the Gauss hypergeometric function.

[29]We have used the relation (see pp. 556, 559 of Ref. 32):

$$F(a,b;c;z)=(1-z)^{-a}\frac{\Gamma(c)\Gamma(b-a)}{\Gamma(b)\Gamma(c-a)}F\left(a,c-b;a-b+1;\frac{1}{1-z}\right)+(1-z)^{-b}\frac{\Gamma(c)\Gamma(a-b)}{\Gamma(a)\Gamma(c-b)}F\left(b,c-a;b-a+1;\frac{1}{1-z}\right)$$

and the fact that, in the small-z approximation, $F(a,b;c;z)=1+O(z)$.

[30]The production mechanism for model I treats all the particles along the multiperipheral chain in a uniform way. The production mechanism for model II treats the end particles differently from the other particles in the inner part of the multiperipheral chain. In the case of form factors, there is some indication that a distinction exists between the momentum-transfer dependence of the end particles as compared to the particles produced from the inner links. [See, e.g., R. C. Hwa, Phys. Rev. D 8, 1331 (1973), and C. B. Chiu *et al.*, *ibid.* 10, 2853 (1974).] In any case, we believe that it is reasonable for us to consider both possibilities here.

[31]I. S. Gradshteyn and I. M. Ryzhik, *Table of Integrals, Series and Products* (Academic, New York, 1965), 4th edition.
[32]M. Abramowitz and I. A. Stegun, *Handbook of Mathematical Functions* (National Bureau of Standards, Washington, D. C., 1964).
[33]D. P. Roy and R. G. Roberts, Nucl. Phys. B77, 240 (1974).
[34]R. D. Field and G. C. Fox, Nucl. Phys. B80, 367 (1974).
[35]M. Hossain, Ph.D. dissertation, The University of Texas at Austin, 1978 (unpublished), and paper in preparation.
[36]M. L. Goldberger, in *Relations de dispersion et particules élémentaires*, edited by C. deWitt and R. Omnès (Hermann, Paris, 1960), p. 50. Also, J. Finkelstein and M. Jacob, Nuovo Cimento 56A, 681 (1968).
[37]H. P. Stapp, Phys. Rev. D 3, 3177 (1971). For application of Steinmann's relation to multiparticle amplitudes, see for example, J. H. Weis, Phys. Rev. D 5 1043 (1972).